

The decay of the neutron-rich nucleus ^{216}Bi

The ISOLDE Collaboration⁴

J. Kurpeta^{1,2}, A. Andreyev², J. Äystö³, A.-H. Evensen⁴, M. Huhta³, M. Huyse², A. Jokinen³, M. Karny¹, E. Kugler⁴, J. Lettry⁴, A. Nieminen³, A. Płochocki¹, M. Ramdhané⁵, H.L. Ravn⁴, K. Rykaczewski^{1,4,6}, J. Szerypo^{1,4}, P. Van Duppen², G. Walter⁵, A. Wöhr²

¹ Institute of Experimental Physics, Warsaw University, Hoża 69, 00681 Warsaw, Poland

² Instituut voor Kern-en Stralingsfysica, University of Leuven, Celestijnenlaan 200D, 3001 Leuven, Belgium

³ Department of Physics, Accelerator Laboratory, University of Jyväskylä, 40351 Jyväskylä, Finland

⁴ ISOLDE, CERN-PPE, 1211, Geneva 23, Switzerland

⁵ Institut de Recherches Subatomiques et Université Louis Pasteur, 67037 Strasbourg, France

⁶ ORNL Physics Division, Oak Ridge, TN 37830, USA

Received: 13 July 1999 / Revised version: 22 September 1999

Communicated by D. Schwalm

Abstract. The decay of the neutron-rich isotope ^{216}Bi , produced by proton-induced spallation at the PS Booster-ISOLDE facility, was investigated by $\beta - \gamma\gamma$, $\alpha\gamma$ coincidence and spectrum-multiscaling measurements. A new method for reducing isobaric contamination enabled to cover the unknown region "east" of ^{208}Pb for the isobaric chain $A=216$. The half-life of the β decay of ^{216}Bi was found as $T_{1/2} = 135 \pm 5$ s. Its decay scheme was extended and the possible shell model configurations are proposed.

PACS. 23.20.Lv Gamma transitions and level energies – 27.80.+w $190 \leq A \leq 219$ – 29.30.Kv X- and γ -ray spectroscopy

1 Introduction

The doubly-magic ^{208}Pb ($Z=82$, $N=126$) nucleus can be considered as a textbook example to illustrate the predictive power of the nuclear shell model. Furthermore ^{208}Pb and nuclei in its neighborhood serve as anchors to fix certain parameters of different models. Therefore vast, but still incomplete, amounts of experimental information exists and several theoretical descriptions are available. The same holds to a certain extent for neutron-deficient nuclei along the $Z=82$ closed shell where phenomena like shape coexistence have been discovered and are of current interest [1,2]. This situation contrasts strongly with the nuclei along the same $Z=82$ closed shell but on the neutron-rich side (east of ^{208}Pb on the chart of nuclides), although the structure of these nuclei is expected to be very rich due to the specific interaction of neutron orbitals (with $N > 126$) with proton orbitals around the $Z=82$ shell closure. Due to the extreme N to Z ratio, these nuclei are hardly accessible with light- or heavy-ion induced fusion reactions. The only possibility seems to fragment heavier actinide targets or beams. Recently the projectile fragmentation of 1000 MeV/nucleon ^{238}U in combination with in-flight separation has been used to study 9 known and 4 new μs isomers in the trans-lead region [3]. The presence of these isomers indicate the prominent role that the high j -orbitals such as $\nu i_{13/2}$, $\nu g_{9/2}$, $\nu j_{15/2}$ and $\pi h_{11/2}$ play. Decay studies at on-line mass separators have been ham-

pered in the past by the overwhelming presence of isobaric contamination in the sources induced by the specific production mechanism.

At the ISOLDE on-line mass separator, a new method has been developed to produce relatively pure sources of these isotopes making use of the pulsed release of the radioactivity. The $A=216$ contaminating isotopes of Rn, Fr and Ra disintegrate by alpha decay with a very short half-lives (in the sub-ms to μs range) whereas the half-life of ^{216}Bi is expected to be in the range of seconds. The PS Booster proton beam has a pulsed structure as described in the next section and due to the thermal diffusion of the reaction products from the target, the release of the produced isotopes is delayed with respect to the beam impact. Thus by blocking the mass separator beam during the beam impact and for a certain time after it, the short-living contaminants have decayed. Details on this technique can be found in [4]. In this paper we report on a β -decay study of ^{216}Bi to excited levels in the even-even ^{216}Po nucleus. Previously there were two transitions of 419 and 550 keV [5] known in the decay scheme of ^{216}Bi , and its half-life was given as 6.6(2.1) minutes in [6] and 3.6(0.4) minutes in [5].

2 Experimental procedure

A 55 g/cm² thick target of $^{232}\text{ThC}_2$ was bombarded with a beam of 1 GeV protons delivered by the PS Booster dur-

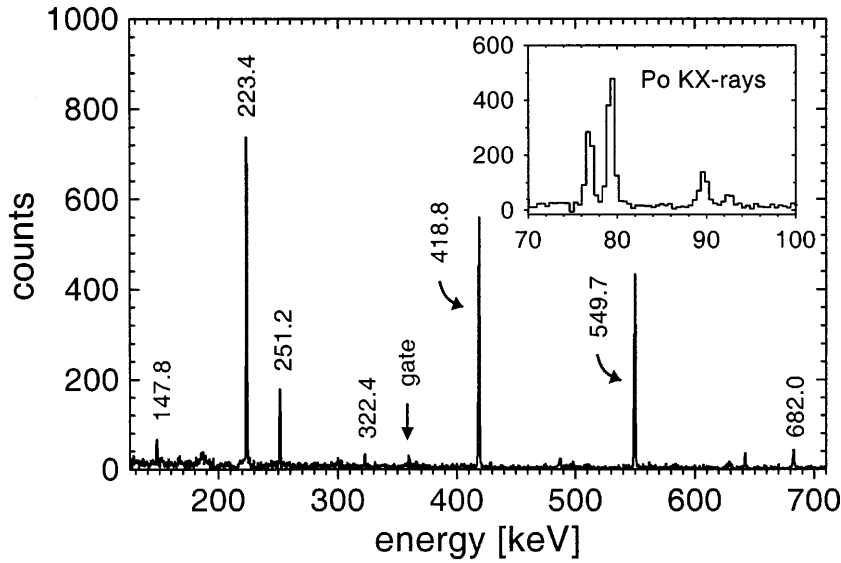


Fig. 1. The γ spectrum taken with the LEGe detector coincident with 359.5 keV line of ^{216}Bi . The region of KX-rays is shown in the inset. Energies are given in keV

ing a 14.4 second supercycle consisting of 12 equidistant pulses with an intensity of 2.8×10^{13} particles per pulse. Radioactive species were produced by using 6 pulses from 2 consecutive supercycles. The target was connected to a hot plasma ion source [7], and the extracted ion beam was mass separated by using the ISOLDE general purpose separator. The beam was finally implanted onto an aluminised mylar tape in front of a detection system. In order to reduce the isobaric contamination the separator beam was interrupted for 200 ms after every proton pulse. The 2 supercycles long (28.8 s) implantation was followed by a 56 s beam-off period.

The data acquisition was blocked during the implantation period, thus only registering radiation during the 56 s beam-off period in an event-by-event as well as in a single spectra mode. The latter contained all the events registered by the α and γ detectors in a 8×7 s multiscaling cycle recorded as disk files whereas coincidence data were stored in list-mode files on a magnetic tape. Data in coincidence mode were recorded if any two of the detectors registered an event simultaneously. The collection tape was moved after every implantation-decay cycle to reduce the background counts coming from unwanted long-living activity. The detector system consisted of a 450 mm^2 , $500 \mu\text{m}$ thick silicon detector for detecting α particles emitted by the contaminants, placed 10.5 mm from the source, a 3850 mm^2 , 20 mm thick LEGe-type germanium detector with a $300 \mu\text{m}$ beryllium window for detecting low energy X- and γ -rays, and a large germanium detector with an efficiency of 60% for 1.3 MeV γ -rays, relative to a $3'' \times 3''$ NaI detector. There was a 0.5 mm thin β plastic scintillator placed between the collection tape and the LEGe detector. The silicon and plastic detectors were used to distinguish beta-delayed or alpha-delayed radiation from background and the isomeric cascades. The detectors were arranged in a close geometry.

3 Experimental results

Energies, coincidence relations and intensities of the observed γ -rays are presented in Table 1. They were attributed to the β -decay of ^{216}Bi on the basis of their half-life and coincidence relations amongst them and with Po KX-rays. All observed coincidences are prompt, indicating life-times of less than 30 ns.

An example of a gated γ spectrum obtained by means of the γ - γ coincidence technique is given in Fig. 1. These kind of spectra allowed us to obtain the coincidence data listed in Table 1. Characteristic X-ray radiation shown in the inset enabled the identification of the coincident tran-

Table 1. Energies, relative intensities (from the LEGe detector single spectrum) and coincidence relations for γ -rays observed in the decay of ^{216}Bi . Superscripts abcd stand for $K_{\alpha 1}$, $K_{\alpha 2}$, $K_{\beta 1,3}$, $K_{\beta 2}$ characteristic X-rays of Po. The γ -intensities were not corrected for summing

E_{γ} [keV]	I_{γ}^{rel} [%]	Coincident γ -lines
147.8	5.6(3)	223.3, 359.9, 418.4, 549.8
223.4	73.2(6)	76.5 ^b , 79.4 ^a , 89.8 ^c , 92.5 ^d , 147.9, 251.3, 322.3, 359.4, 418.8, (428.3), 549.8, 682.4
251.2	19.1(4)	224.0, 360.0, 419.4, 549.9
322.4	3.7(3)	223.5, 359.4, 418.9, 549.6
359.5	81.2(8)	76.9 ^b , 79.3 ^a , 89.7 ^c , 92.5 ^d , 147.9, 223.5, 251.3, 418.8, 549.8, 682.6
418.8	93.1(9)	76.8 ^b , 79.4 ^a , 89.8 ^c , 92.4 ^d , 147.9, 223.5, 251.3, 322.4, 359.5, 549.8, 682.8
428.7	1.7(3)	(223.7), 360.0, 419.1, 550.7
486.9	4.5(4)	223.3, 359.5, 419.1, 549.9
549.7	100(1)	76.9 ^b , 79.3 ^a , 89.8 ^c , 92.6 ^d , 147.9, 223.5, 251.2, 359.5, 418.9, 487.5, 682.7
682.0	7.5(4)	76.7 ^b , 79.4 ^a , 89.5 ^c , 91.7 ^d , 223.5, 359.2, 418.7, 550.0

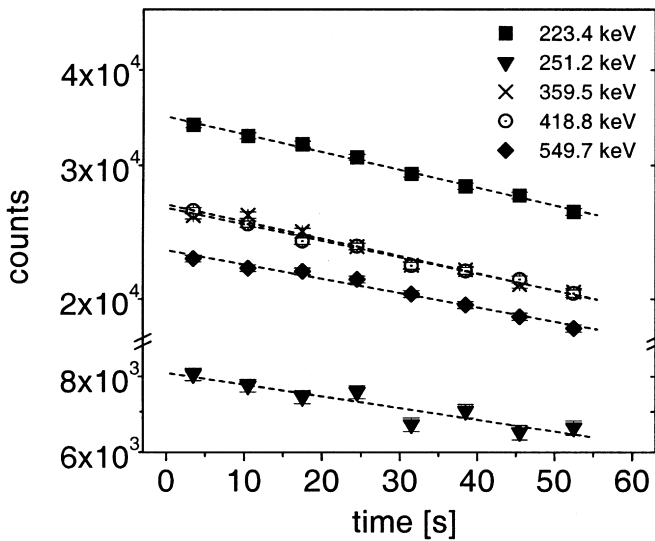


Fig. 2. Decay of the selected gamma lines recorded with the LEGe detector in single spectra mode for ^{216}Bi

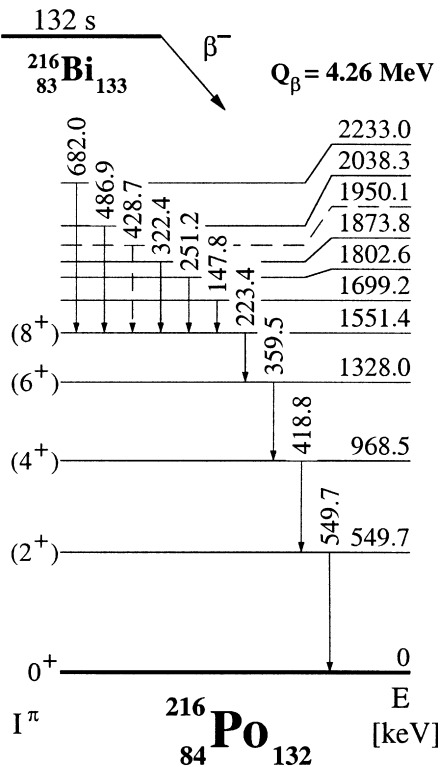


Fig. 3. The decay scheme of ^{216}Bi

sitions of Fig. 1 occurring in ^{216}Po . The decay curves in logarithmic scale for some of the γ transitions associated with the decay of ^{216}Bi are shown on Fig. 2.

The half-life value for ^{216}Bi was determined from the multiscale data to be $T_{1/2} = 135 \pm 5$ s which is significantly different from the previously reported half-lives of 6.6(2.1) minutes [6] and 3.6(0.4) minutes [5]. The intensity of the γ -lines from long-lived activity in the different multispectrum subgroups was constant. Therefore

no dead-time correction was applied. There were only the two lowest transitions 550 keV and 419 keV observed before in ^{216}Po with intensities 100% and 44% respectively [5]. Together with the mentioned discrepancy in the lifetimes, this points to the existence of two β -decaying states in ^{216}Bi . A longer-living low-spin state as observed in the previous studies [5,6] and a shorter-living high-spin state discussed here. In the discussion of Ruchowska *et al.*, they conclude that the level at 969 keV, deexciting by the 419 keV γ -line to the 2^+ level in ^{216}Po at 550 keV, has most probably 0^+ , 1^+ or 2^+ as spin and parity. As will become more clear below our data contradicts this assignment. A possible explanation of the conflicting results could be the fact that a different admixture of the two beta-decaying states is present in the three experiments: only the low-spin state in the experiment of Burke *et al.* as its selectively fed in the α decay of the low spin ground state of ^{220}At [8], a mixture in the case of Ruchowska *et al.*, [5] and almost a pure high-spin state population in the present work as will be discussed below. The half-life of 3.6 ± 0.4 min measured by Ruchowska *et al.* lies in between the value of 6.6 ± 2.1 min obtained by Burke *et al.* and our value of 135 ± 5 s which provides further proof for this assumption. In the experiments of Burke *et al.* and of Ruchowska *et al.* the radioactive species were produced by spallation reaction of ^{232}Th target induced by 600 MeV and 200 MeV protons respectively. The products were separated using the on-line mass separator ISOLDE II in the former and ISOCELE II in the latter case. It is not clear what causes the different population probabilities.

The β decay scheme of ^{216}Bi , based on the coincidence relations shown in Table 1 and on the systematics of the lighter Po isotopes, is shown in Fig. 3. The Q_β value is taken from theory [9]. The two strong γ lines at 223 and 360 keV together with the already known 419 and 550 keV lines [5] seem to form a cascade which leads, by assuming stretched E2 transitions, to an 8^+ state in ^{216}Po .

With the experimental setup at our disposal it was not possible to verify multiplicities of the investigated transitions. Except for the stretched E2 cascade no reliable assumptions on the multiplicities of the other transitions can be made, and thus $\log ft$ values are difficult to calculate.

4 Discussion

4.1 Possible ground state and isomer configurations in the odd-odd Bi isotopes above N=126

The most probable configuration of the ground state of the odd-odd Bi isotopes with $N > 126$ is formed by the odd proton in the $1h_{9/2}$ shell and the odd neutron in the $2g_{9/2}$, shell leading to a multiplet with spin and parity ranging from 0^- to 9^- . By applying the parabolic rule described by Paar in [10] it is possible to calculate the energies between the members of the multiplet. Using as coupling constants 40 MeV/A and 4 MeV for the dipole and quadrupole interaction, respectively, the parabola changes

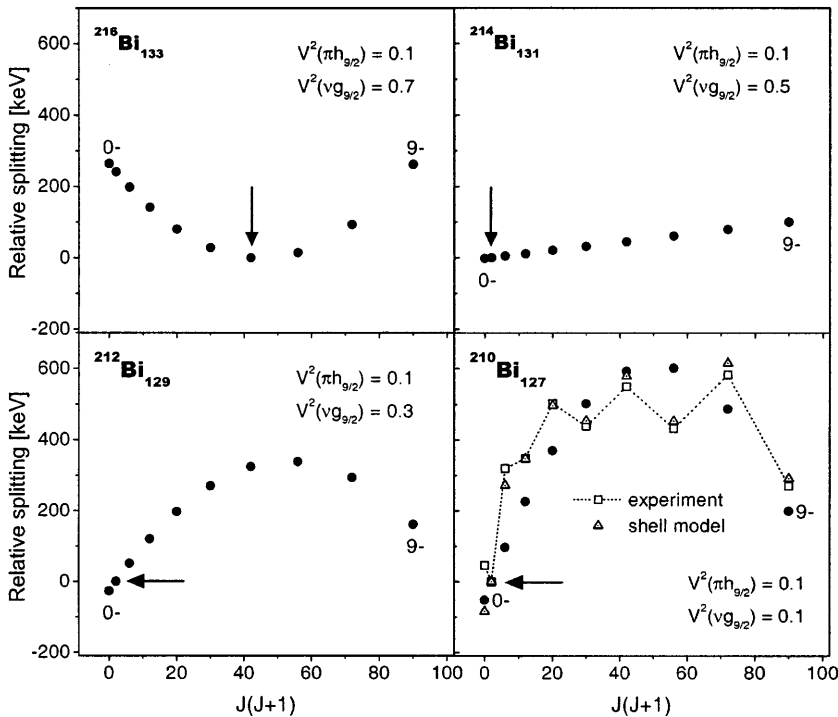


Fig. 4. The full dots present the relative energy splittings predicted with a parabolic rule of [10] (normalized to 0 keV at the points indicated by arrows). For ^{210}Bi compared to experimental data [11] and shell model predictions [12]

from upwards bend (^{210}Bi , ^{212}Bi) over almost flat (^{214}Bi) to downwards bend (^{216}Bi) as the number of particles in the $\nu 2g_{9/2}$ shell increases from 1 to 7 (see Fig. 4). This would lead to isomerism in $^{210,212}\text{Bi}$ (0^- and 9^-), to a low-spin ground state in ^{214}Bi (0^- or 1^-) and to a high spin ground state in ^{216}Bi (6^- or 7^-). The validity of this simple prescription can be estimated for ^{210}Bi where the multiplet splitting according to Paar is compared with experiment [11] and with shell model calculations using the Kuo-Herling interaction [12]. Indeed for ^{210}Bi and ^{212}Bi the 1^- level becomes the ground state while the 9^- state is isomeric and decays by alpha and/or beta decay. In ^{214}Bi [13] only the 1^- ground state is β decaying while from our work it is clear that the main beta decay comes from a high-spin state as most of the intensity arrives at the 8^+ level.

From the time behaviour of the γ lines attributed to the decay of ^{216}Bi (see Fig. 2), the intensity balance of the $8^+ - 6^+ - 4^+ - 2^+ - 0^+$ cascade (resp. 73%, 81%, 93% relative to 100% for the $2^+ - 0^+$ transition) and an estimate of the influence of conversion and missing γ -rays it is not possible to decide if we do observe in this experiment the β decaying low-spin state of ^{216}Bi .

4.2 The level structure of the even-even Po isotopes

The low-lying levels in the even-even Po isotopes are governed firstly by the two-proton particle degrees of freedom and secondly by the interaction of these two protons outside the $Z=82$ closed shell with the valence neutrons. The $N=126$ closed shell nucleus ^{210}Po shows only the first type of interaction, and is thus a classical example of a doubly-closed shell nucleus plus two particles. The excited levels

can be described as two-proton excitations such as the broken pair configurations $\pi(1h_{9/2})^2$ leading to 2^+ , 4^+ , 6^+ , 8^+ excited states, $\pi(1h_{9/2}, 2f_{7/2})$ leading to a $1^+ - 8^+$ multiplet and $\pi(1h_{9/2}, 1i_{13/2})$ leading to a $2^- - 11^-$ multiplet. Warburton and Brown [12] have used the Kuo-Herling interaction to perform shell-model calculations for ^{210}Po . They nicely reproduce the experimental energies and can trace down the dominant configurations in the excitation spectrum of ^{210}Po . They conclude that the low-lying $8^+ - 6^+ - 4^+ - 2^+ - 0^+$ cascade involves mainly the $\pi(1h_{9/2})^2$ configuration. The $\pi(1h_{9/2}, 2f_{7/2})$ multiplet ranges from 2.19 MeV to 2.38 MeV while the $\pi(1h_{9/2}, 1i_{13/2})$ multiplet ranges from 2.85 MeV to 3.09 MeV.

Recently the systematics of even-even light Po isotopes with $N \leq 126$ (see Fig. 5) have been discussed in an extensive way [14]. The heavier Po isotopes ($A \geq 202$) can be described by the two interactions given above leading to collective effects well described by the Particle-Core model. From ^{200}Po on a $4p - 2h$ proton intruder configuration mixes in with the regular structure and leads eventually in ^{192}Po to a deformed ground state [14].

Very little is known about the even-even Po isotopes above $N=126$ shell closure (see Fig. 5) but the picture emerging shows clear differences to the one below the neutron shell closure (see Table 2). Similarly to the 2 neutron-hole nucleus ^{208}Po , the 2 neutron-particle nucleus ^{212}Po has a first excited 2^+ state which is considerably lower than the 2^+ state in the closed neutron shell nucleus ^{210}Po . But in contrast to the $N < 126$ Po nuclei where the 2^+ energy remains constant until ^{200}Po , the first excited 2^+ state decreases further when adding neutron pairs. The well known isomerism based on the small energy difference between the 8^+ and 6^+ member of $\pi(1h_{9/2})^2$ multi-

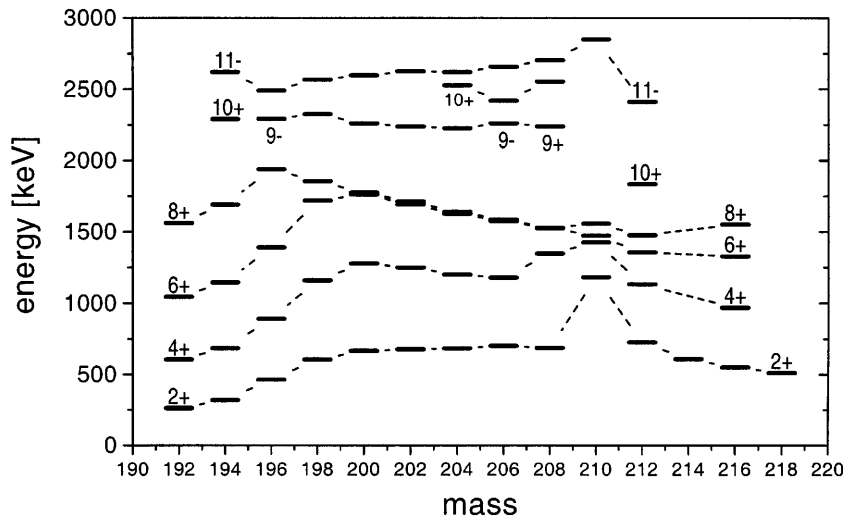


Fig. 5. Selected energy levels in even-even Po isotopes. Based on [15] [16] [17] and this paper

Table 2. Energies in keV of the first excited 2^+ states (E_{2^+}) and energy differences between the 8^+ and 6^+ states (ΔE) for the even-even Po isotopes

A	192	194	196	198	200	202	204	206	208	210	212	214	216	218
E_{2^+}	262	319	463	605	666	677	684	701	687	1181	727	609	550	511
ΔE	518	545	549	136	12	20	12	13	4	94	122	–	223	–

plet which is present from ^{208}Po on until ^{200}Po is not at all seen above the $N=126$ shell closure. A possible explanation could be related to the huge differences in orbitals occupied by the neutrons below and above the $N=126$. Indeed, below the $N=126$ shell closure the neutron holes are first in the $3p_{1/2}$, $2f_{5/2}$ and $3p_{3/2}$ shells which give little possibility to build up angular momentum higher than 4. Only for neutron numbers in the neighborhood of $N=114$ the high $i_{13/2}$ neutron orbital starts to play a role. Above $N=126$, the neutron occupy high-spin orbitals such as $2g_{9/2}$, $1j_{15/2}$ and $1i_{11/2}$; breaking these neutron pairs will lead to multiplet structures which will interact with the $\pi(1h_{9/2})^2$ multiplet.

4.3 Properties of the states fed in the ^{216}Bi decay

As stated already above, it is hard to obtain absolute β feeding intensities as conversion could change drastically the total intensities involved. The number of X-rays coincident with the four transitions in the 8^+ to 0^+ cascade indicate indeed that some of the γ rays feeding the 8^+ state are considerably converted. However this surplus can not be taken in a quantitative way into account as the exact feeding pattern is not known. Furthermore our decay scheme is probably not complete as our sensitivity for γ rays in the energy range between 100 and 700 keV is 50 times lower than that for the 2^+ to 0^+ transition. For energies around 1500 keV this is even 120 times lower. Taking all this into account the β feeding pattern emerging from our decay scheme is that all feeding occurs to or above the 8^+ state, although no direct feeding to the 6^+ state can be excluded, and this with $\log ft$ values between 6.2 and

7.3. The possible allowed or first forbidden β decay modes of the $\pi 1h_{9/2} \times \nu(2g_{9/2})^7$ ground state of ^{216}Bi leads to $\pi(1h_{9/2})^2$, $\pi(1h_{9/2}, 2f_{7/2})$ and $\pi(1h_{9/2}, 1i_{13/2})$ configurations with the valence neutrons in the $\nu(2g_{9/2})^6$ configuration. The other excitations have either much higher energy or are much more forbidden in beta decay, and their population requires a mixed configuration in initial and/or final states.

Considering the limitations from Q_β window and taking into account the position of the three broken proton multiplets as observed in ^{210}Po (see Sect. 4.2) we expect to have the main feeding towards the $\pi(1h_{9/2})^2$ based states although the interaction with the valence neutrons in the $2g_{9/2}$ orbital could split up the strength. The fact that the main intensity in the ground state band (β and γ feeding) occurs to the 8^+ level is a striking experimental fact and could point to a 9^- ground state of ^{216}Bi , in contradiction with the parabolic rule, or could point to specific configurations in the 8^+ and 6^+ states. Further experimental evidence, including electron spectroscopy together with theoretical efforts are needed to clarify this point.

5 Conclusions

The β decay of ^{216}Bi has been studied and, apparently due to high spin of the ^{216}Bi ground state, levels in ^{216}Po are observed up to 8^+ . Candidates for the broken $\pi(1h_{9/2})^2$ pair are proposed which makes it possible to follow this broken pair excitation in the even-even Po isotopes from neutron number 108 over the closed-shell at $N=126$ up to $N=132$. Above the $N=126$ closure this broken pair is

less stable than below indicating the role of the valence neutrons occupying high j-orbitals.

References

1. J.L. Wood *et al.*, Phys. Rep. **215**, (1992) 103
2. K. Heyde *et al.*, Phys. Rep. **102**, (1983) 291
3. M. Pfützner *et al.*, Phys. Lett. **B444**, (1998) 32
4. P. Van Duppen *et al.*, Nucl. Instr. Meth. **B134**, (1998) 267
5. E. Ruchowska *et al.*, J. Phys. **G16**, (1990) 255
6. D.G. Burke *et al.*, Z. Phys. **A333**, (1989) 131
7. J. Lettry *et al.*, Nucl. Instr. Meth. **B126**, (1997) 130
8. A. Artna-Cohen, Nucl. Data Sheets **80**, (1997) 157
9. P. Möller *et al.*, At. Data Nucl. Data Tables **59**, (1995) 185
10. V. Paar, Nucl. Phys. **A331**, (1979) 16
11. R.K. Sheline *et al.*, Czech. J. Phys. **B39**, (1989) 22
12. E.K. Warburton, B.A. Brown, Phys. Rev. **C43**, (1991) 602
13. Y.A. Akovali, Nucl. Data Sheets **76**, (1995) 127
14. A.M. Oros *et al.*, Nucl. Phys **A645**, (1999) 107
15. K. Helariutta *et al.*, Phys. Rev. **C54**, (1996) 2799
16. W. Younes *et al.*, Phys. Rev. **C52**, (1995) 1723
17. R.B. Firestone, *Table of Isotopes – 8th ed.* (John Wiley & Sons, Inc., New York, 1996)